

## GEODETTIC ESTIMATE OF COSEISMIC SLIP DURING THE 1989 LOMA PRIETA, CALIFORNIA, EARTHQUAKE

M. Lisowski, W. H. Prescott, J. C. Savage, and M. J. Johnston

U.S. Geological Survey, Menlo Park, California

**Abstract.** Offsets in the relative positions of geodetic stations resulting from the Loma Prieta earthquake can be explained with a dislocation model that includes buried oblique slip on a rupture surface extending 37 km along the strike of the San Andreas fault, dipping 70° to the SW, and extending from a depth of about 5 to 17.5 km. Assuming uniform slip on a rectangular surface, the mean values for a range of reasonable fault geometries are  $1.6 \pm 0.3$  m right-lateral strike slip and  $1.2 \pm 0.3$  m reverse slip. Slip on an adjacent extension of the rupture to the southeast, recorded in the aftershock sequence, is not well constrained by the geodetic data. The geodetic data clearly preclude rupture extending near the surface.

## Introduction

The Loma Prieta earthquake (October 17, 1989;  $M_s = 7.1$ ) ruptured a part of the San Andreas fault where surface deformation has been monitored with an extensive and frequently measured geodetic network (Figure 1). Although widespread secondary surface cracking was associated with the earthquake, there was no tectonic surface rupture [U.S. Geological Survey Staff, 1990]. The coseismic changes in the relative positions of the geodetic stations provide a means of estimating the slip on the buried fault rupture.

The geodetic data set we use consists primarily of precise electronic distance measurements (EDM), with a few Global Positioning System relative position changes (GPS is a radio interferometric technique of obtaining relative positions) and two Very Long Baseline Interferometry (VLBI) position changes. The characteristics of the EDM and GPS systems are described below, and the VLBI measurements are described by Clark *et al.* [1990].

The U.S. Geological Survey (USGS) has observed the distance between a set of permanent geodetic stations in the San Francisco bay area since the early 1970's [Prescott *et al.*, 1981]. Distances are measured with a Geodolite, a laser distance measuring instrument. Aircraft measurements of atmospheric temperature and humidity and ground measurements of pressure are used to correct for variations in the refractive index of light. The precision obtained with these techniques is about 0.2 ppm [Savage and Prescott, 1973]. Some lines are measured with a short-range distance meter (HP 3808) using end-point meteorology and have a precision of about 2 ppm. Geodolite surveys were conducted at

intervals from one to five years. Three Geodolite lines (Loma to Eagle Rock, Allison, and Hamilton) have been measured monthly since 1981 [Lisowski *et al.*, 1990].

In 1985, the monthly Geodolite observations from the top of Loma Prieta mountain were supplemented by monthly GPS observations of all three components of the position vectors between Loma and the stations Allison and Eagle Rock. In 1988 and 1989 the position vectors between Loma and the stations Hamilton and Brush 2 were measured several times. The precision of these observations is also 0.2 ppm, although the precision obtained depends on the orientation of the line and the techniques used to process the data [Prescott *et al.*, 1989; Davis *et al.*, 1989].

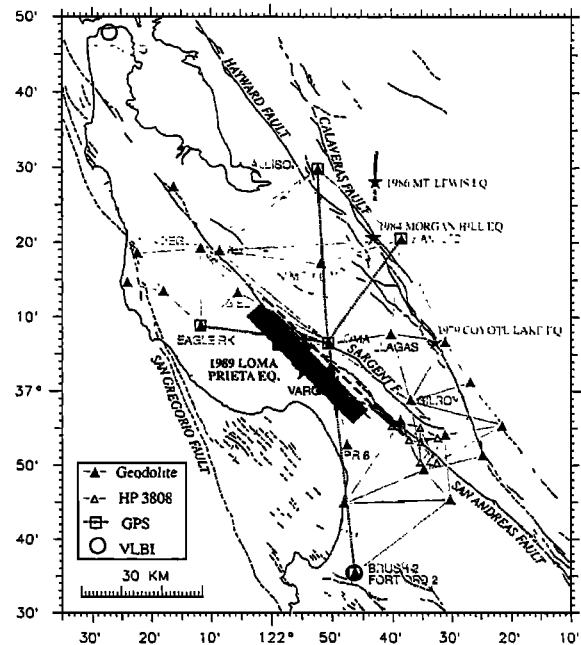


Fig. 1. Map of southern San Francisco Bay area showing major faults [Jennings, 1975], the epicenters (stars) and rupture zones (shaded) of the Loma Prieta earthquake and several other recent earthquakes, and the Geodolite, HP 3808, GPS, and VLBI stations. The surface projections of the buried model faults for the Loma Prieta earthquake are outlined with shaded rectangles, and the heavy dashed line shows where these faults would intersect the surface.

This paper is not subject to U.S. copyright. Published in 1990 by American Geophysical Union.

Paper number 90GL01565  
0094-8276/90/90GL-01565\$03.00

A subset of these lines and vectors has been remeasured since the earthquake. We use the observed coseismic change to infer the magnitude, direction, and distribution of slip that occurred during the earthquake. In this paper, we will discuss the observations and present a preliminary model for the coseismic slip distribution.

## Analysis

## Preprocessing

Ideally, we would like to have an observation of each line immediately before and after the earthquake. Then the coseismic change would simply be the difference between the two observations. The GPS and Geodolite observations from station Loma come close to that ideal. There were GPS observations on October 6 and October 19, and Geodolite observations on October 3 and October 19. However, other stations were not observed as frequently. Secular change in the line length can be substantial, and it was necessary to employ a technique that separated the secular change from the coseismic change.

Our experience indicates that the secular change in line length can be very well modeled as a linear function of time. Consequently, for most lines, we fit a model that included three parameters, a slope and intercept (*i.e.*, a straight line) plus an offset on October 17th. Additional offsets were included for lines affected by 1979 Coyote Lake earthquake ( $M_L = 5.9$ , see *King et al.* [1981] for details), the 1984 Morgan Hill earthquake ( $M_L = 6.2$ , see *Prescott et al.* [1984] for details), or the 1986 Mt. Lewis earthquake ( $M_L = 5.9$ ) (epicenters and rupture zones shown in Figure 1). The slope, intercept, and coseismic offsets were determined by a weighted least squares fit to the observations of each line or vector component.

In this manner, we obtained an estimate of the coseismic change on October 17th for 84 Geodolite lines and 4 GPS vectors. Coseismic position change of the VLBI stations Fort Ord 2 (located near Brush 2), Presidio, and Point Reyes were estimated in a similar way by *Clark et al.* [1990]. The estimated uncertainty in this change is equal to the larger of the experimental uncertainty based on prior estimates of the uncertainty of individual measurements or the theoretical uncertainty derived from the weighted least squares fit. Most coseismic changes at station Loma are listed in Table 1.

Note that this model assumes that the secular rate after the earthquake is the same as that before the earthquake. If there are significant postseismic slip, visco-elastic relaxation, or longer-term effects on the strain field [*e.g.*, *Thatcher*, 1983], this assumption may be invalid. Little postseismic change has been observed in the lines and vectors measured several times in the months after the earthquake. The clearest case for postseismic deformation is the observation of a few millimeters of slip across the San Andreas fault north of the Loma Prieta rupture zone [*Langbein*, 1990].

## Modeling

Coseismic slip on the fault surface was calculated by fitting a dislocation model for the rupture to the observed line length and vector component changes. The Earth was modeled as an elastic half space and the rupture as slip on a dipping rectangular cut buried in the half space [*Mansinha and Smylie*, 1967]. The slip was allowed to have both dip and strike slip components. A least squares inversion was used to select the amount of right-lateral and reverse slip most consistent with the observed earthquake offsets.

The geometry of the starting fault model was based on the locations of the main shock and aftershocks [*Dietz and*

Table 1. Coseismic Offsets at Station Loma

Line	$L$ km	$\Delta L_{eq}$ , mm	Calc. mm	$o-c$ mm
<i>Geodolite</i>				
american loma	19.7	$-66.5 \pm 7.8$	-23.1	-43.4
biel loma	25.4	$235.4 \pm 11.6$	229.6	5.8
bmt rf loma	35.4	$176.2 \pm 18.1$	115.6	60.6
loma mindego	39.2	$175.0 \pm 12.8$	128.5	46.5
allison loma	43.1	$109.0 \pm 8.0$	95.0	14.0
eagle rk loma	31.5	$259.7 \pm 5.8$	242.8	16.9
hamilton loma	31.2	$51.1 \pm 6.0$	69.2	-18.1
loma pr6	26.0	$-273.9 \pm 10.1$	-293.2	19.3
loma lp2	5.7	$-40.9 \pm 5.2$	-29.1	-11.8
loma lp4	6.6	$-212.0 \pm 7.9$	-218.0	6.0
loma vargo	11.4	$-204.0 \pm 15.3$	-285.8	81.8
<i>GPS*</i>				
north loma allison	-43.2	$-109.6 \pm 4.0$	-92.3	-17.3
east loma allison	2.4	$36.9 \pm 11.0$	2.9	34.0
up loma allison	0.2	$-105.6 \pm 29.9$	-138.2	32.6
north loma eagle rk	-4.8	$-205.9 \pm 5.1$	-203.7	-2.2
east loma eagle rk	31.2	$212.2 \pm 8.7$	222.9	-10.7
up loma eagle rk	0.3	$-209.8 \pm 23.6$	-230.6	20.8
north loma hamilton	-25.7	$-104.4 \pm 4.8$	-94.0	-10.4
east loma hamilton	-17.9	$58.6 \pm 8.5$	21.5	37.1
up loma hamilton	-0.2	$-120.6 \pm 26.5$	-129.8	9.2

\*Listed are the components ( $L$ ) and earthquake related changes ( $\Delta L_{eq}$ ) of the relative position vector (*e.g.*, (north loma<sub>post</sub> - north allison<sub>post</sub>) - (north loma<sub>pre</sub> - north allison<sub>pre</sub>)).

*Ellsworth*, 1990]. The main shock had a focal depth of 17.6 km. The aftershocks defined a 45-km-long zone trending N50°W, extending from depths of 4 to 18 km, and dipping 65° to the southwest. Aftershocks in the southeastern 10 km of the rupture were on a near-vertical plane aligned with the San Andreas fault and extended to a depth of only 10 km. We tried models with one dipping segment and models with a dipping segment and an adjacent near-vertical segment that slipped independently. The model fault geometry was then altered by trial and error to minimize the difference between the observed and calculated offsets.

## Discussion

## Results of Dislocation Modeling

Most of the observed coseismic deformation can be explained by oblique slip ( $1.66 \pm 0.05$  m right-lateral strike slip and  $1.19 \pm 0.06$  m reverse slip) on a 37-km-long buried rupture surface extending from a depths of 5 to 17.5 km and dipping 70° to the southwest (Table 2, model 3). The uncertainties in the slip estimates are conditional uncertainties based solely on the data uncertainty. A more realistic assessment would scale these uncertainties by the misfit of the model (2.4) and by uncertainty in the model geometry. A reasonable range of slip values are those given for the Models 2, 3, and 4 with the tops at 4, 5, and 6 km. The mean values for these models are  $1.6 \pm 0.3$  m right-lateral strike slip and  $1.2 \pm 0.3$  m reverse slip on the dipping segment. The geodetic moment ( $M_0 = \mu Ab$ , where  $\mu$  is the rigidity—a value

Table 2. Dislocation Model Geometry, Calculated Slip, and Misfit to Geodetic Data

Model	Strike	Dip SW	Top km	Bottom km	Width km	Length km	Strike Slip m	Reverse Slip m	Misfit <sup>1</sup>	Moment N-m
1	N44°W	70°	2.0	17.5	16.5	37	0.82 ± 0.04	0.46 ± 0.04	4.4	1.8 × 10 <sup>19</sup>
2	N44°W	70°	4.0	17.5	14.4	37	1.36 ± 0.04	0.88 ± 0.05	2.7	2.6 × 10 <sup>19</sup>
3	N44°W	70°	5.0	17.5	13.3	37	1.66 ± 0.05	1.19 ± 0.06	2.4	3.0 × 10 <sup>19</sup>
4	N44°W	70°	6.0	17.5	12.2	37	1.98 ± 0.06	1.53 ± 0.08	2.7	3.4 × 10 <sup>19</sup>
5 NW	N44°W	70°	5.0	17.5	13.3	37	1.59 ± 0.05	1.17 ± 0.06	2.3	2.8 × 10 <sup>19</sup>
5 SE	N50°W	85°	3.0	9.0	6.0	10	0.74 ± 0.20			0.1 × 10 <sup>19</sup>

<sup>1</sup> The weighted rms of residuals divided by the number of degrees of freedom. Values greater than 1.0 imply that data noise is not sufficient to explain the residuals.

of  $3 \times 10^{10}$  Pa was used,  $A$  is the area of the slip zone, and  $b$  the slip) is  $3.0 \times 10^{19}$  N-m. The strike (N44°W), dip (70°SW), and rake (144°) of this buried rupture as estimated from the geodetic data agrees with the main shock mechanism (strike N50° ± 10°W, dip 70° ± 15°SW, rake 140° [Oppenheimer, 1990]).

The optimum location for the northwestern edge of the rupture describes a dipping plane nearly coincident with the aftershocks, with its updip surface projection located two kilometers northeast of the surface trace of the San Andreas fault (Figure 1). The optimum location of the southeastern edge of the dipping fault, however, is two km southwest of plane defined by the aftershocks.

Allowing slip on a 10-km-long near-vertical extension to the southeast provided a slightly better fit to the data (Table 2, Model 5), but the amount of slip ( $0.74 \pm 0.20$  m right-lateral strike slip) and model geometry were poorly constrained. In this two-segment model, the model parameters for the northwestern dipping fault were roughly the same as those in the one-segment model.

The geodetic data are consistent with other possibilities for the rupture geometry, such as a kinked rupture zone [Dietz and Ellsworth, 1990, Figure 6]. Models 3 and 5 given in Table 2 are simply the best of the simple uniform slip models we tested, but they are not unique. These models provide a preliminary estimate of the coseismic slip distribution. In the near future, releveling and additional GPS observations may shed further light on the slip during the event.

#### Observed and Calculated Displacements

The misfit of the model to the data can be judged by comparing the observed and predicted coseismic station displacements (Figure 2). The combination of VLBI, GPS, and EDM provides a unique solution of the displacement field within the geometrically rigid part of the network. For stations with weak ties (*e.g.*, LP 2, LP 4) the indeterminate components of the displacement field are fixed by minimizing the difference between their computed values and the values predicted by the model (using the "model coordinate" solution of Segall and Matthews [1988]). Such a solution results in degenerate error ellipses (lines at the end of the vectors) when there is insufficient information to fix both components of the displacement field. The fit of the model to the data is acceptable with most of the predicted displacements being within the 95% confidence limit of the observed displacements. The solution could, no doubt, be improved

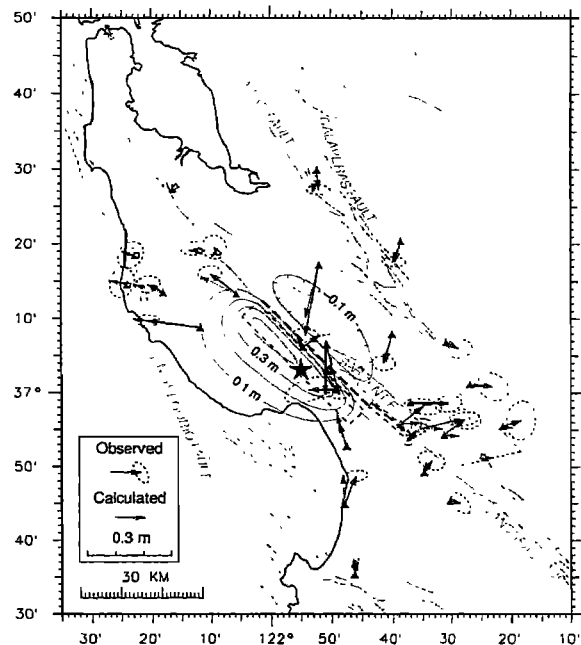


Fig. 2. Map showing the observed station displacements (solid arrows) and the station displacements predicted by the dislocation model (dashed shaded arrows). The observed displacements are tipped with a 95% confidence interval error ellipse. See text for description of the particular solution shown. The surface projections of the model faults are outlined with dashed rectangular boxes, and the heavy dashed line shows where the updip projection of these faults would intersect the surface. Contours show the elevation change predicted by the dislocation model.

with a more complex model of the rupture geometry and slip distribution. The pure error, estimated from the misclosure in this geometrically redundant network, is 1.2 times the prior error, whereas the misfit of the model is 2.3 times the prior error.

The data most poorly fit by the model comes from stations in the epicentral area (Loma, LP2, LP4, Vargo), station American, and the stations between the Calaveras and the San Andreas faults southeast of the rupture. Given the widespread surface fractures and secondary faulting observed in the epicentral area [U.S. Geological Survey Staff, 1990], it is

likely that some of the motions of stations near the epicenter may be due to local movements.

The only direct measure of elevation change reported here comes from the GPS vectors to Loma (Table 1). It is interesting to note that Loma Prieta, the highest peak in the Santa Cruz Mountains, subsided about 0.1 m relative to Allison and Hamilton and about 0.2 m relative to Eagle Rock. Elevation change predicted by the dislocation model is shown in Figure 2.

#### *Absence of surface rupture*

It is quite clear from Table 2 that the geodetic observations are best fit with a rupture that terminates well short of the Earth's surface. The lengths of lines Loma-LP2 and Loma-LP4, which cross the San Andreas fault near the epicenter, changed only a fraction of a meter (Table 1) even though the total slip was nearly 2 m. These results are quite consistent with the absence of any surface expression of primary rupture. There has been some discussion in the literature concerning the question of how much slip occurred along this section of the fault in the 1906 San Francisco earthquake. Thatcher and Lisowski [1987] inferred from triangulation observations that the average slip from the surface to 10 km was  $2.6 \pm 0.2$  m. Based primarily on an observation of an apparent fault offset in the summit railway tunnel south of Wright's station [Lawson, 1908], Scholz [1985] and others have argued that the slip along this section in 1906 was 1.5 m, significantly less than farther north along the peninsula. It has been argued that this section of the fault must rupture more frequently to make up the slip deficit that was "observed" in 1906. The occurrence of the Loma Prieta earthquake seems to give support to this argument. In 1989, however, no surface slip was observed, bringing into question whether surface slip is a valid criteria for earthquake prediction along this section of the San Andreas fault.

*Acknowledgements.* Immediately after the earthquake, we received valuable field assistance from K. Hudnut, F. Webb, and S. Larsen, of the California Institute of Technology and from M. Jackson of the University of Colorado. We thank Donna Eberhart-Phillips and Wayne Thatcher of the U.S.G.S. for their careful reviews. Bob Mueller of the USGS provided the trilateration data for the HP 3808 network.

#### References

- Clark, T. A., C. Ma, J. M. Sauber, J. W. Ryan, D. Gordon, D. B. Shaffer, D. S. Caprette, and N. R. Vandenberg, Geodetic measurement of deformation in the Loma Prieta, California, earthquake with very long baseline interferometry, *Geophys. Res. Lett.*, in press, 1990.
- Davis, J. L., W. H. Prescott, J. L. Svarc, and K. L. Wendt, Assessment of Global Positioning System measurements for studies of crustal deformation, *J. Geophys. Res.*, **94**, 1365-13650, 1989.
- Dietz, L., and W. L. Ellsworth, The October 17, 1989, Loma Prieta, California, earthquake and its aftershocks: Geometry of the sequence for high-resolution locations, *Geophys. Res. Lett.*, in press, 1990.
- Jennings, C. W., Fault map of California, with locations of volcanoes, thermal springs, and thermal wells: California Division of Mines and Geology, *Geologic Data Map 1*, scale 1:750,000, 1975.
- King, N. E., Savage, J. C., Lisowski, M., and Prescott, W. H., Preseismic and coseismic deformation associated with the Coyote Lake, California, earthquake, *J. Geophys. Res.*, **86**, 13635-13650, 1989.
- Langbein, J. O., Postseismic slip on the San Andreas fault at the northwestern end of the Loma Prieta earthquake, *Geophys. Res. Lett.*, in press, 1990.
- Lawson, A. C., The California Earthquake of April 18, 1906, *Report of the State Earthquake Investigation Commission*, Carnegie Inst. of Wash., Wash., D.C., **1**, 109-113, 1908.
- Lisowski, M., W. H. Prescott, J. C. Savage, and J. L. Svarc, A possible geodetic anomaly observed prior to the Loma Prieta, California, earthquake, *Geophys. Res. Lett.*, in press, 1990.
- Mansinha, L., and D. E. Smylie, The displacement fields of inclined faults, *Bull. Seism. Soc. Am.*, **61**, 1433-1440, 1967.
- Oppenheimer, D., Aftershock slip behavior of the 1989 Loma Prieta, California, earthquake, *Geophys. Res. Lett.*, in press, 1990.
- Prescott, W. H., M. Lisowski, J. C. Savage, Geodetic measurement of crustal deformation across the San Andreas, Hayward, and Calaveras faults near San Francisco, California, *J. Geophys. Res.*, **86**(B11), 10853-10869, 1981.
- Prescott, W. H., N. E. King, and G. H. Gu, Preseismic, coseismic, and postseismic deformation associated with the 1984 Morgan Hill, California, earthquake, *Calif. Div. Mines and Geol., Sp. Pub. 68*, 137-148, 1984.
- Prescott, W. H., J. L. Davis, and J. L. Svarc, Global positioning system measurements for crustal deformation: Precision and accuracy, *Science*, **244**, 1337-1340, 1989.
- Savage, J. C., W. H. Prescott, Precision of Geodolite distance measurements for determining fault movements, *J. Geophys. Res.*, **78**, 6001-6008, 1973.
- Scholz, C. H., The Black Mountain asperity: Seismic hazard of the southern San Francisco peninsula, California, *Geophys. Res. Lett.*, **12**, 717-719, 1985.
- Segall, P., and Matthews, M. V., Displacement calculations from geodetic data and the testing of geophysical deformation models, *J. Geophys. Res.*, **93**, 14,954-14,966, 1988.
- Thatcher, W., Nonlinear strain buildup and the earthquake cycle on the San Andreas fault, *J. Geophys. Res.*, **88**, 5893-5902, 1983.
- Thatcher, W., and M. Lisowski, Long-term potential of the San Andreas fault southeast of San Francisco, California, *J. Geophys. Res.*, **92**, 4771-4784, 1987.
- U.S. Geological Survey Staff, The Loma Prieta, California, earthquake: an anticipated event, *Science*, **247**, 286-293, 1990.
- M. J. Johnston, M. Lisowski, W. H. Prescott, and J. C. Savage, U.S. Geological Survey, Menlo Park, CA 94025.

(Received: April 10, 1990;

Revised: July 9, 1990;

Accepted: July 9, 1990.)